Dissociation Kinetics of Echinomycin from CpG Binding Sites in Different Sequence Environments[†]

Michael C. Fletcher[‡] and Keith R. Fox*

Department of Physiology & Pharmacology, University of Southampton, Bassett Crescent East, Southampton SO16 7PX, U.K.

Received October 2, 1995; Revised Manuscript Received November 20, 1995[⊗]

ABSTRACT: We have examined the kinetics of dissociation of echinomycin from CpG sites in several DNA fragments containing synthetic DNA inserts by a variation of the footprinting technique. Complexes of the ligand with radiolabeled DNA fragments were dissociated by adding an excess of unlabeled calf thymus DNA. Samples were removed from this mixture at subsequent time intervals and subjected to DNase I footprinting. The rate of disappearance of the footprints varied considerably between the various CpG sites. At 20 °C, echinomycin dissociates more slowly from CpG sites flanked by $(AT)_n$ ($t_{1/2} \sim 40$ min) and $(CA)_n{\cdot}(TG)_n$ ($t_{1/2} \sim 11$ min) than by $A_n{\cdot}T_n$ ($t_{1/2} < 3$ min). In each sequence context the dissociation from ACGT is slower than that from TCGA. $(TAA)_4CG(TTA)_4$ also represents a very good binding site ($t_{1/2} \sim 35$ min), which is less sensitive to changes in temperature than most other sites. Within sequences $(AT)_{10}(G/C)_4(AT)_{10}$, the dissociation from CGGC is slower than that from CCCG or CCGC.

Echinomycin is an antitumor antibiotic possessing a cyclic octadepsipeptide, to which are attached two quinoxaline chromophores, which is known to bind to DNA by bifunctional intercalation (Waring & Fox; 1983, Waring, 1990) and unwind DNA by 48°. It has long been known to bind best to GC-rich DNAs (Wakelin & Waring, 1976). Various footprinting (Low *et al*., 1984; Van Dyke & Dervan, 1984; Bailly *et al*., 1994), NMR (Gao & Patel, 1988; Gilbert & Feigon, 1991, 1992; Gilbert *et al*., 1989), and X-ray crystallographic studies (Wang *et al*., 1984, 1986; Ughetto *et al*., 1985; Quigley, 1986) on echinomycin and the closely related compound triostin have shown that they are selective for the dinucleotide CpG. Specificity is achieved by the formation of hydrogen bonds between the 2-amino group of guanine and the carbonyl oxygens of the alanines and between the guanine N3 and alanine NH groups. The requirement for the purine 2-amino group has been confirmed by experiments in which guanine has been replaced by inosine, thereby abolishing binding (Marchand *et al*., 1992; Addess & Feigon, 1994a), or in which adenine has been replaced with 2,6-diaminopurine, generating new echinomycin binding sites (Bailly *et al*., 1993; Waring & Bailly, 1994; Bailly & Waring, 1995). As well as unwinding DNA, all of the X-ray structures have shown that the bases adjacent to the intercalated chromophore adopt Hoogsteen rather than Watson−Crick base pairing. However, it seems that this structure does not form in longer DNA fragments (McLean & Waring, 1988; Sayers & Waring, 1993), and several NMR studies with short oligonucleotides have shown that the induction of Hoogsteen base pairing depends on the flanking bases (Gao & Patel, 1988; Gilbert & Feigon, 1991, 1992; Addess & Feigon, 1994b).

Although there have been numerous studies on DNA sequence recognition by these antibiotics, little is known about the kinetics of their interaction with DNA. This information is important since, for a related series of compounds, there is often a correlation between biological activity and persistence time on the DNA lattice (dissociation rate constant). Early studies used SDS sequestration to measure the dissociation of echinomycin and other quinoxaline antibiotics from binding sites in bulk DNA samples (Fox *et al*., 1981; Fox & Waring, 1981). In this technique, a complex between a ligand and DNA is dissociated by adding SDS (final concentration up to 2%), which sequesters the ligand as it dissociates from DNA; this process is usually measured by changes in the absorbance. It was found that the dissociation from natural DNAs requires at least three exponentials for its complete description, in contrast to synthetic DNAs, such as poly(dG−dC), for which the reaction was completely described by a single-exponential decay. This was explained by suggesting that the multiexponential decay from mixed-sequence DNA represents the parallel dissociation of the ligand from different binding sites on the lattice, each of which possesses its own microscopic dissociation rate constant. The relative amplitude of the slowest component ($t_{1/2} \sim 10$ min) increased at lower binding ratios, consistent with the suggestion that it represents dissociation from the strongest binding sites. Although these studies reveal useful information about the dissociation process, they can only provide average dissociation parameters for natural DNAs that contain a large number of potential sites and cannot reveal the identity of the best binding sites. Although the fastest dissociating components must represent the interaction of the ligand with weaker sites, it is not clear whether these correspond to non-CpG sites or a subset of CpG sites with lower affinity. Indeed the dissociation from poly(dG−dC) is faster than that of the

[†] This work was supported by a grant from the Biotechnology and Biological Sciences Research Council.

* Corresponding author: telephone, +1703-594374; fax, +1703-594319.

[‡] Present address: Dept. of Biochemistry, University of Saskatchewan, Saskatoon, Saskatchewan S7N OWO, Canada.

[⊗] Abstract published in *Advance ACS Abstracts,* January 1, 1996.

0006-2960/96/0435-1064$12.00/0

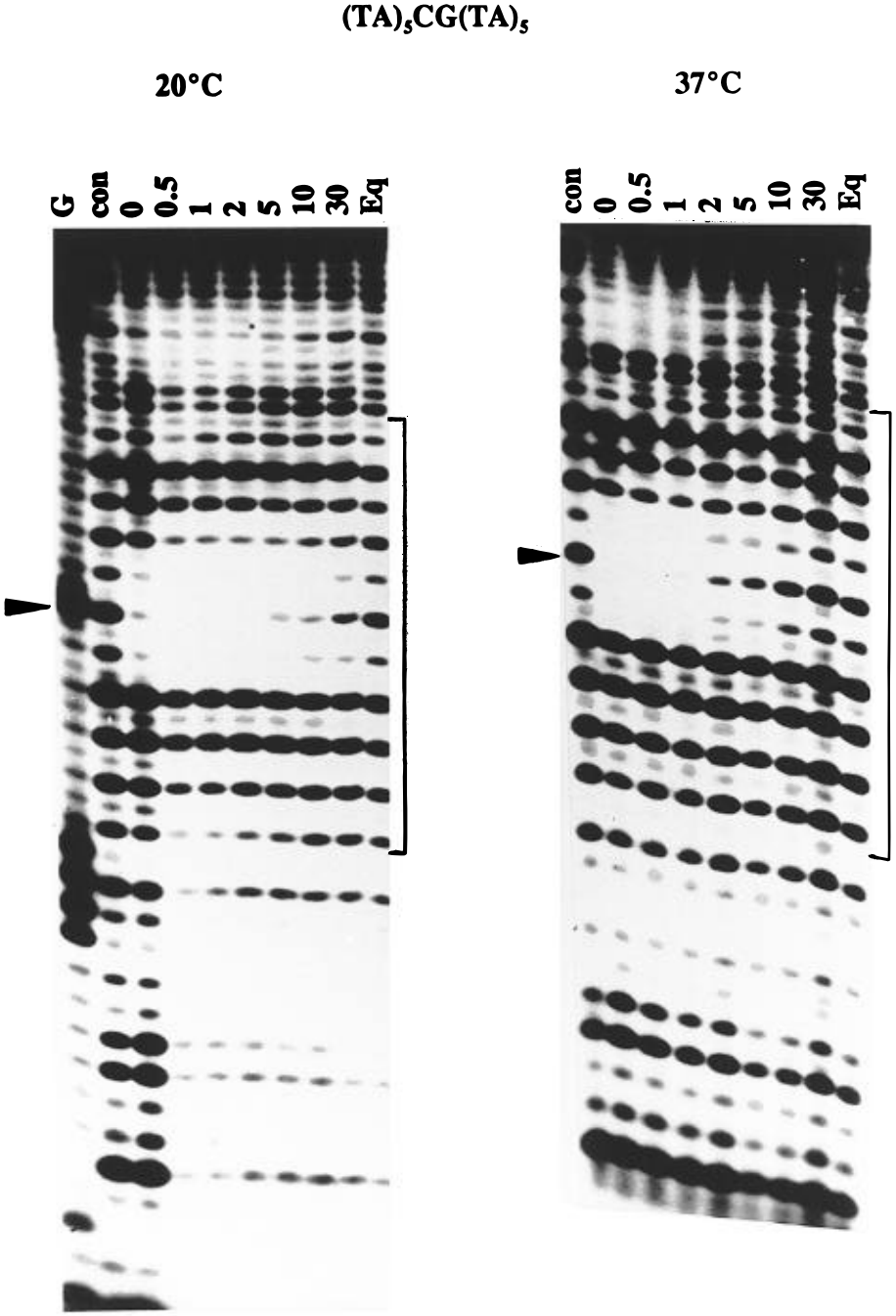

FIGURE 1: DNase I digestion patterns showing the dissociation of 20 μM echinomycin from a DNA fragment containing the insert $(TA)_5CG(TA)_5$, measured at 20 and 37 °C. Aliquots were removed from the mixture at various times after adding the unlabeled calf thymus DNA and subjected to short (12 s) digestion by DNase I. The time after adding the competitor DNA (minutes) is indicated at the top of each lane. con indicates digestion of the DNA alone in the absence of any ligand; 0 corresponds to digestion of a complex with 20 μM echinomycin before adding the unlabeled DNA. In the track labeled Eq, the labeled and unlabeled DNAs were mixed before adding the ligand and represent the true equilibrium distribution of the ligand in the dissociating mixture. The track labeled G is a Maxam−Gilbert dimethyl sulfate−piperidine marker specific for guanine. The arrows indicate the position of the guanines in each CpG site; the square brackets show the position and length of the insert.

slowest component from natural DNAs (Fox *et al.*, 1981), suggesting that GCGC may not represent the best binding site. Leroy *et al*. (1992) confirmed the slow dissociation of echinomycin by measuring amide proton exchange rates for the depsipeptide, estimating a half-life of 20 min at 15 °C. In addition, several studies on the inhibition of transcription by echinomycin have shown that the dissociation rates can vary considerably between different CpG sites (White & Phillips, 1989a,b; Phillips *et al*., 1990).

There have been several SDS dissociation studies with actinomycin using short oligonucleotides. These reveal that the rate of dissociation from each GpC site depends on the nature of the surrounding bases (Chen, 1988a,b, 1990, 1992). In general, actinomycin dissociates faster from GC sites that are preceded by G or followed by C than from other sites such as AGCA, AGCG, or CGCA. The dissociation from ATATGCATAT is unusually slow ($t_{1/2}$ = 3000 s), while GGCC represents one of the fastest GpC sites (Chen, 1988a).

We have recently developed a modification of the footprinting technique for examining the dissociation of ligands from individual binding sites on mixed-sequence DNA (Fletcher & Fox, 1993). In this technique, a complex

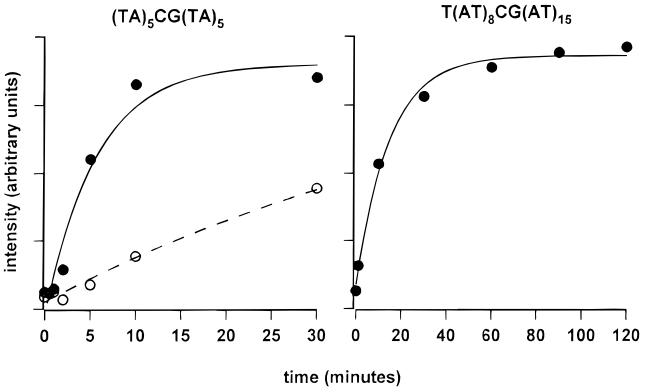

FIGURE 2: Rate of dissociation of echinomycin from $(TA)_5CG(TA)_5$ and $T(AT)_8CG(AT)_{15}$. The left-hand panel shows the rate of dissociation from $(TA)_5CG(TA)_5$. The data are taken from densitometer scans of the autoradiographs presented in Figure 1. The ordinate shows the intensity of bands corresponding to cleavage of the central GpT step, normalized with respect to the intensity of the second GpG step immediately below the insert. The filled circles show the rate of dissociation at 37 °C and are fitted by the solid line with a decay constant of 0.18 ± 0.05 min^{-1}. The open circles show the dissociation at 20 °C and are fitted by the dashed line with a decay constant of 0.017 ± 0.001 min^{-1}. The right-hand panel shows the data for $T(AT)_8CG(AT)_{15}$, derived from densitometer scans of the autoradiographs presented in Figure 3. The ordinate represents the intensity of bands corresponding to cleavage of the second ApT step below the central CpG (i.e., CGATAT) normalized with respect to the intensity of the band corresponding to cleavage of the sixth ApT step from the bottom of the insert, which is not affected by echinomycin binding. The curve fitted to the data points is a single exponential with a decay constant of 0.068 ± 0.009 min^{-1}.

between the ligand and a radiolabeled DNA fragment is dissociated by adding a vast excess of unlabeled calf thymus DNA. Aliquots are removed from the dissociation mixture at various times after the competitor DNA is added and are subjected to DNase I footprinting. The dissociation is visualized by the rate of disappearance of the footprinting pattern. By using this technique, we have shown that actinomycin dissociates from each of its binding sites in *tyr*T DNA at different rates (Fletcher & Fox, 1993) and have examined the dissociation of TANDEM, a synthetic quinoxaline antibiotic, from its TpA binding sites (Fletcher *et al.*, 1995). In this paper, we have used the modified footprinting technique to examine the dissociation of echinomycin from CpG sites that are located in different sequence environments. The interaction of echinomycin with several of the fragments, and its effects on their structure, has been previously described (Waterloh & Fox, 1991; Fox *et al.*, 1991).

MATERIALS AND METHODS

Drugs and Enzymes. Echinomycin was obtained from the U.S. National Cancer Institute and stored at 4 °C as a 1 mM stock solution in dimethyl sulfoxide. This was diluted to working concentrations in 10 mM Tris-HCl (pH 7.5) containing 10 mM NaCl immediately before use. DNase I was purchased from Sigma and stored at −20 °C at a concentration of 7200 units/mL. All other enzymes were purchased from Promega. [α-^{32}P]dATP (3000 Ci/mmol) was purchased from Amersham.

DNA Fragments. The preparation of pUC plasmids containing synthetic DNA inserts $T(AT)_8CG(AT)_{15}$, $T_{15}CGA_{15}$, $[(TAA)_4CG(TTA)_4]_2$, $(AT)_{10}CCCG(AT)_{10}$, $(AT)_{10}CGGC(AT)_{10}$, and $(AT)_{10}CCGC(AT)_{10}$ has been previously described (Waterloh & Fox, 1991; Fox *et al.*, 1991; Carpenter *et al.*, 1993). In each case, the insert was cloned into the *Sma*I site of the polylinker. Plasmids containing the inserts $[(CA)_5CG(TG)_5]_2$ and $(TA)_5CG(TA)_5$ were prepared for this work in a similar manner by cloning the self-complementary oligonucleotides (prepared on an Applied Biosystems DNA synthesizer) into the *Sma*I site of pUC19. Successful clones were picked from agar plates containing X-Gal and IPTG as white colonies, and their sequences were checked using a T7 Sequencing kit (Pharmacia). Radiolabeled polylinker fragments containing the inserts were prepared by digesting with *Hin*dIII, labeling the 3′-end with [α-^{32}P]dATP using reverse transcriptase, and digesting again with *Eco*RI. Radiolabeled fragments of interest were separated from the remainder of the plasmid on 7% (w/v) polyacrylamide gels.

Table 1: Rate Constants for the Dissociation of Echinomycin from Various DNA Fragments, Estimated from the Rate of Disappearance of DNase I Footprints

	k (min^{-1})	
sequence	20 °C	37 °C
$(TA)_5CG(TA)_5$	0.017 ± 0.001	0.18 ± 0.05
$T(AT)_8CG(AT)_{15}$	0.068 ± 0.009	1.15 ± 0.62
$T_{15}CGA_{15}$[a]	0.214 ± 0.005	
$[(TAA)_4CG(TTA)_4]_2$		
lower site	0.022 ± 0.005	0.086 ± 0.015
upper site	0.023 ± 0.006	0.068 ± 0.013
$[(CA)_5CG(TG)_5]_2$		
lower site	0.064 ± 0.020	0.199 ± 0.033
upper site	0.059 ± 0.186	0.32 ± 0.08
$(AT)_{10}CGGC(AT)_{10}$	0.087 ± 0.010	

[a] Estimated by using diethyl pyrocarbonate modification.

DNase I Footprinting. Samples for footprinting were prepared by mixing 9 μL of radiolabeled DNA (about 50 pmol of base pairs) with 9 μL of echinomycin at a concentration of 20−100 μM in 10 mM Tris-HCl (pH 8.0) containing 10 mM NaCl. This mixture was left for at least 30 min to ensure equilibration of the drug and DNA. Dissociation of the antibiotic from the DNA was initiated by adding 10 μL of calf thymus DNA (3 mM base pairs). Aliquots (4 μL) were removed from this mixture at various times and digested with 2 μL of DNase I (150 units/mL dissolved in 2 mM $MgCl_2$, 2 mM $MnCl_2$, and 20 mM NaCl). The digestion reaction was stopped after 12 s by the addition of 4 μL of formamide containing 10 mM EDTA and 0.1% (w/v) bromophenol blue. The footprinting pattern of the mixture at equilibrium was determined by mixing the radiolabeled DNA with calf thymus DNA before the addition of the antibiotic and digesting in the same manner. Digestion patterns of the native DNA and the complex before dissociation were obtained in the usual manner by mixing 1.5 μL of radiolabeled DNA with 2 μL of drug and digesting for 1 min with 2 μL of DNase I (0.03 unit/mL).

Diethyl Pyrocarbonate Modification. Radiolabeled DNA (9 μL) was mixed with 9 μL of ligand, and dissociation was initiated by the addition of 10 μL of unlabeled calf thymus DNA, as described earlier for the experiments with DNase I. Reaction mixture (7 μL) was removed at the appropriate times and added to 5 μL of diethyl pyrocarbonate. The reaction was allowed to proceed for 5 min with gentle agitation before it was stopped by the addition of 0.3 M

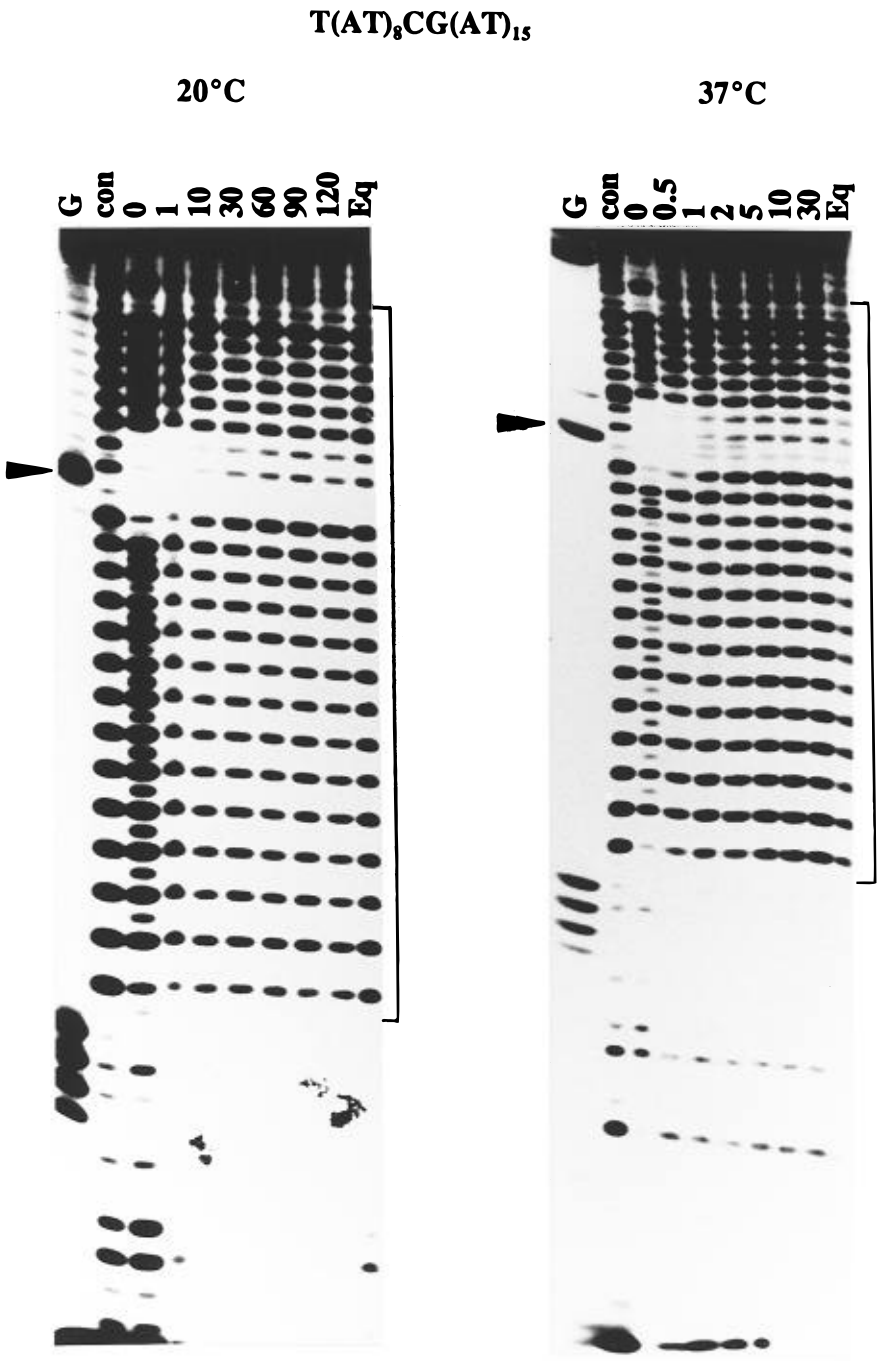

FIGURE 3: DNase I digestion patterns showing the dissociation of 20 μM echinomycin from a DNA fragment containing the insert $T(AT)_8CG(AT)_{15}$ measured at 20 and 37 °C. The time after adding the competitor DNA (minutes) is indicated at the top of each lane. con indicates digestion of the DNA alone in the absence of any ligand; 0 corresponds to digestion of a complex with 20 μM echinomycin before adding the unlabeled DNA. In the track labeled Eq, the labeled and unlabeled DNAs were mixed before adding the ligand and represent the true equilibrium distribution of the ligand in the dissociating mixture. Tracks labeled G are Maxam−Gilbert dimethyl sulfate−piperidine markers specific for guanine. The arrows indicate the position of the guanines in the CpG sites; the square brackets show the position and length of the insert.

sodium acetate. The DNA was precipitated with 70% ethanol, washed twice with 70% ethanol, and dried. The pellet was then boiled in 50 μL of 10% piperidine (v/v) for 15 min before drying and resuspension in 7 μL of formamide containing 10 mM EDTA.

Gel Electrophoresis. All samples were heated to 95 °C for 3 min prior to electrophoresis. The products of digestion were resolved on 8% (w/v), 40 cm long polyacrylamide gels containing 8 M urea. Gels were run at 1500 V for about 2 h. They were then fixed in 10% acetic acid, transferred to Whatmann 3MM paper, dried under vacuum at 80 °C, and subjected to autoradiography at −70 °C with an intensifying screen. Bands in the digests were assigned by comparison with Maxam−Gilbert dimethyl sulfate−piperidine markers specific for guanine or for guanine and adenine or by comparison with previously published digestion patterns. The exposure of the autoradiographs presented has been adjusted so as to highlight the regions of interest. Gels were scanned with a Hoefer 365W scanning microdensitometer. The time dependent values for the intensity of the bands were fitted by a single-exponential function using FigP for Windows. In each case, the intensity of the bands of interest within the footprint were normalized by comparison with a band that is not affected by the ligand, outside the footprinting site.

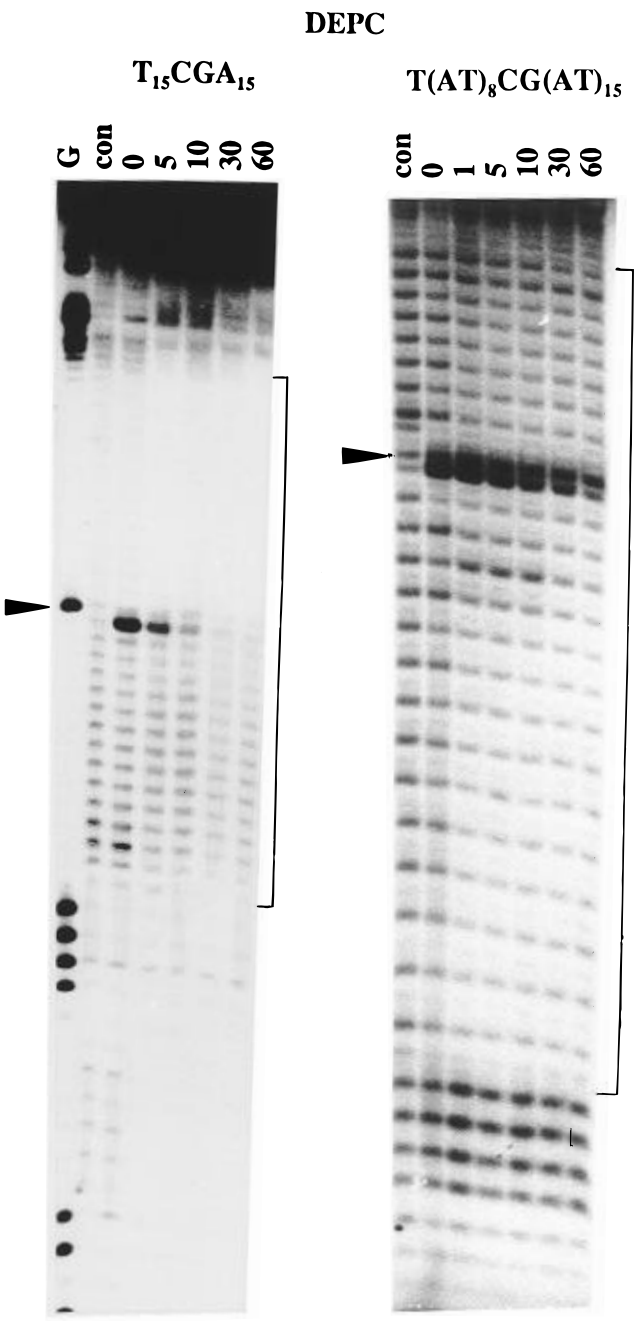

FIGURE 4: Dissociation of 20 μM echinomycin from DNA fragments containing the inserts $T_{15}CGA_{15}$ and $T(AT)_8CG(AT)_{15}$, determined by changes in the reactivity to diethyl pyrocarbonate at 20 °C. Aliquots were removed from the mixture at various times after adding the unlabeled calf thymus DNA and reacted with diethyl pyrocarbonate for 5 min. The time after adding the competitor DNA (minutes) is indicated at the top of each lane. con indicates digestion of the DNA alone in the absence of any ligand; 0 corresponds to digestion of a complex with 20 μM echinomycin before adding the unlabeled DNA. The arrows indicate the position of the guanines at the central CpG sites; the square brackets show the position and length of the inserts.

RESULTS

CG Surrounded by (AT)$_n$. Figure 1 presents the dissociation of echinomycin from a DNA fragment containing the insert $(TA)_5CG(TA)_5$. Cleavage of this fragment in the absence of the ligand produces a pattern in which each of the RY steps (ApT, ApC, and GpT) is cut much better than the intervening YR steps. Echinomycin produces a clear footprint around the central CpG, which covers 6−7 base pairs (lane 0). It can be seen that, upon adding the unlabeled competitor DNA, this footprint disappears in a time dependent fashion. At 20 °C the pattern has hardly changed by 5 min and still resembles the undissociated complex. Cleavage products from the central GpT step begin to reappear after 10 min and have not returned to the control even 30 min after adding the competitor DNA. Lane Eq shows the cleavage pattern obtained when the radiolabeled and competitor DNAs are mixed before adding the echinomycin, generating a true equilibrium distribution of the ligand. From this it can be seen that, at equilibrium, the cleavage pattern is very similar to that in the control, confirming that there is sufficient competitor DNA to ensure almost complete dissociation of the complex, which requires longer than 30 min. As expected, the reaction is faster at 37 °C and dissociation is virtually complete by 10 min. To obtain a more quantitative estimate of the dissociation parameters, we have performed a densitometric analysis of these data. We have estimated the intensity of the band corresponding to cleavage of the central GpT at various time points. To correct for variations in gel loading or differences in the extent of digestion of each sample, we have normalized this value by comparing it with the intensity of the cleavage of the second GpG step immediately below the insert, which is not affected by echinomycin binding. The results of this analysis are presented in Figure 2 (left-hand panel). This quantitative analysis yields values for the dissociation rate constants of 0.017 and 0.18 min^{-1} at 20 and 37 °C, respectively. These values, together with the data obtained with other fragments described in the following, are summarized in Table 1. The value at 20 °C ($t_{1/2}$ = 40 min) is slower than the slowest component observed in the dissociation from mixed-sequence DNAs by SDS sequestration; this difference will be considered further in the Discussion.

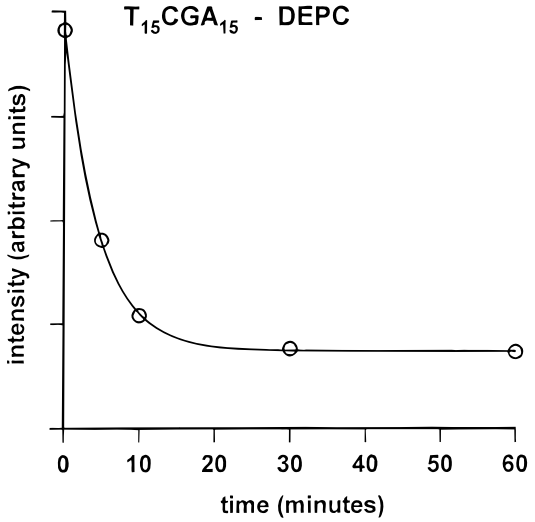

FIGURE 5: Rate of dissociation of echinomycin from $T_{15}CGA_{15}$ measured by changes in the reactivity toward diethyl pyrocarbonate. The data are derived from densitometer scans of the autoradiograph shown in Figure 4. The ordinate shows the intensity of the hyperreactive adenine (CGA) relative to the intensity of an adenine in the center of the A_{15} tract that is not affected by echinomycin binding. The curve fitted to the points corresponds to a single exponential with a decay constant of 0.214 ± 0.005 min^{-1}.

We have compared the dissociation from the tetranucleotide ACGT, described earlier, with the sequence TCGA in a similar environment using the sequence $T(AT)_8CG(AT)_{15}$.

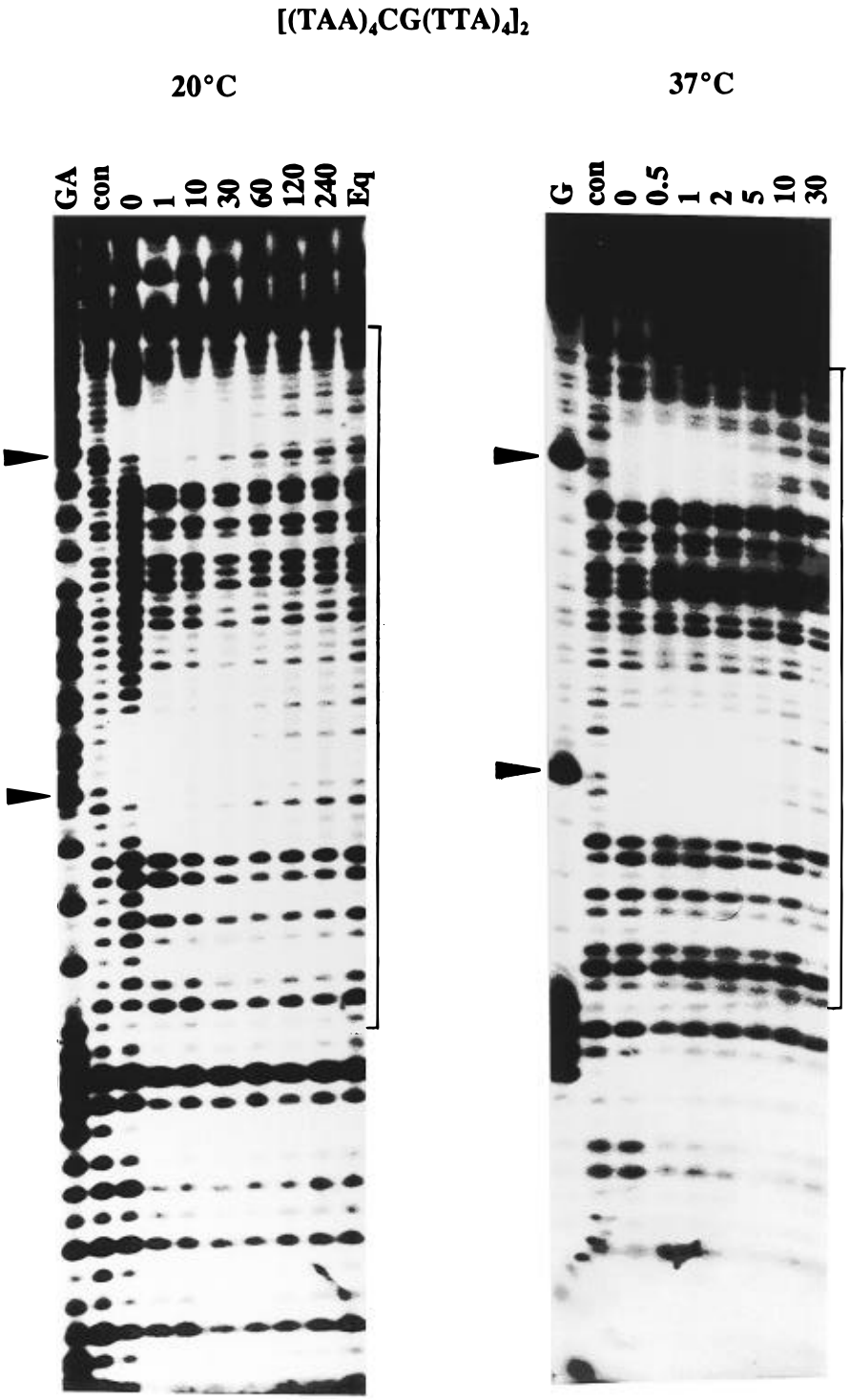

FIGURE 6: DNase I digestion patterns showing the dissociation of 20 μM echinomycin from a DNA fragment containing the dimeric insert $[(TAA)_4CG(TTA)_4]_2$ measured at 20 and 37 °C. The time after adding the competitor DNA (minutes) is indicated at the top of each lane. con indicates digestion of the DNA alone in the absence of any ligand; 0 corresponds to digestion of a complex with 20 μM echinomycin before adding the unlabeled DNA. In the track labeled Eq, the labeled and unlabeled DNAs were mixed before adding the ligand and represent the true equilibrium distribution of the ligand in the dissociating mixture. Tracks labeled G and GA are Maxam−Gilbert dimethyl sulfate−piperidine markers specific for guanine and guanine plus adenine, respectively. The arrows indicate the position of the guanines in the CpG sites; the square brackets show the position and length of the insert.

The results are presented in Figure 3. It can be seen that, once again, the dissociation is slow and at 20 °C is not complete 30 min after adding the competitor DNA. Inspection of the dissociation at 37 °C suggests that it may be slightly faster than that from $(TA)_5CG(TA)_5$ since the bands in the center of the footprint have returned to the control intensity by 2 min, rather than 5 min. We have quantified these data by measuring the intensity of cleavage of the ApT step at the 3′-edge (lower) of the footprint (CGATAT) and normalizing this with respect to the central ApT step, which is not affected by echinomycin binding. The results are presented in the right-hand panel of Figure 2 and are summarized in Table 1. They yield values for the dissociation rate constants of 0.068 and 1.15 min^{-1} at 20 and 37 °C, respectively. These values are about 5-fold faster than the corresponding rates from $(TA)_5CG(TA)_5$, suggesting that, in

an alternating AT environment, ACGT is a better binding site than TCGA.

As previously noted (Waterloh & Fox, 1991; Fox *et al.*, 1991), the DNase I cleavage pattern of the $(AT)_n$ tracts in $T(AT)_8CG(AT)_{15}$ is modified by the antibiotic. This can be seen in the time 0 lane at both 20 and 37 °C as a four-base repeating pattern in which every other TpA step shows increased cleavage in the presence of the antibiotic. Although the precise origin of this unusual pattern remains obscure, it is thought to arise from a weaker interaction of the ligand with the alternating AT tracts, probably by binding to ApT. This is consistent with the observation that echinomycin binds, albeit weakly, to poly(dA−dT) (Wakelin & Waring, 1976) and dissociates from it much faster than from poly(dG−dC) (Fox *et al.*, 1981). This unusual pattern disappears rapidly upon adding the competitor DNA and is no longer evident by the first time point.

CG Surrounded by A_n·T_n and $(TAA)_n$·$(TTA)_n$. Previous studies (Waterloh & Fox, 1991) have shown that echinomycin interacts only weakly with the inserts $A_{15}CGT_{15}$ and $T_{15}CGA_{15}$ and that neither sequence yields clear DNase I footprints. Therefore, it is not possible to employ the preceding protocol, using DNase I, to measure the rate of dissociation from these sequences. However, several studies have shown that echinomycin renders adenines distal to its CpG binding site hyperreactive to diethyl pyrocarbonate (Portugal *et al.*, 1988; McLean & Waring, 1988; Fox & Kentebe, 1990a; Waterloh & Fox, 1991; Fox *et al.*, 1991) and that such hyperreactivity is induced in $T_{15}CGA_{15}$. We therefore have reacted the samples with diethyl pyrocarbonate at various times after the addition of the competitor DNA. It should be noted that this technique is less accurate than use of DNase I as a result of the longer reaction time (5 min) required with diethyl pyrocarbonate than the 12 s routinely employed in the DNase I digestions; during this time there will be further dissociation of the ligand. The results are presented in Figure 4 and show that the intensity of the band corresponding to the hyperreactive adenine (CGA) is markedly reduced by 5 min and is virtually absent 10 min after adding the competitor DNA. A kinetic plot, derived from densitometric analysis of these data, is presented in Figure 5 and yields a dissociation rate constant at 20 °C of 0.21 min^{-1}. Since several studies have shown that enhancements in diethyl pyrocarbonate reactivity persist to lower ligand concentrations than DNase I footprints (Fox & Kentebe, 1990a,b; Waterloh & Fox, 1991), this value cannot be directly compared with DNase I digestion data and should be taken as an upper limit of the dissociation time. Similar experiments with $T(AT)_8CG(AT)_{15}$ are presented in the right-hand panel of Figure 4 and reveal a much slower disappearance of the DEPC enhancements, which are still clearly evident 60 min after adding the competitor DNA. Although it is not possible to directly compare DNase I with diethyl pyrocarbonate data, it is clear that the dissociation of echinomycin from $T_{15}CGA_{15}$ is much faster than that from $T(AT)_8CG(AT)_{15}$. Similar experiments with $A_{15}CGT_{15}$ are not possible since adenines on the 5′-side of the binding site are not rendered hyperreactive to diethyl pyrocarbonate.

Figure 6 presents the dissociation of echinomycin from a DNA fragment containing the dimeric insert of $(TAA)_4CG(TTA)_4$. Previous studies have shown that echinomycin produces clear DNase I footprints on this sequence, in contrast to its sequence isomer $(ATT)_4CG(AAT)_4$, which shows no changes in digestion in the presence of echinomycin (Waterloh & Fox, 1991). It can be seen that the two footprints with $[(TAA)_4CG(TTA)_4]_2$ persist for about 30 min at 20 °C and are still evident after 5 min at 37 °C. Quantitative analyses of bands within the footprints, derived from densitometer traces of these autoradiographs, are presented in Figure 7. These yield average values for the dissociation rate constants of about 0.02 and 0.077 min^{-1} at 20 and 37 °C, respectively (see Table 1). At 20 °C the dissociation rate is similar to that measured with $(TA)_5CG(TA)_5$, while at 37 °C echinomycin dissociates more slowly from $(TAA)_4CG(TTA)_4$ than from $(TA)_5CG(TA)_5$. This difference will be considered further in the Discussion. Additional experiments (not shown) revealed that the dissociation from this fragment is still slow enough to measure at 55 °C, yielding dissociation rate constants of 0.48 ± 0.19 and 0.78 ± 0.15 min^{-1} at the lower and upper sites, respectively. Although previous studies have failed to detect a DNase I footprint with $(ATT)_4CG(AAT)_4$ (Waterloh & Fox, 1991), we noticed a small decrease in DNase I cleavage around the central CpG, which disappeared within 2 min of adding the competitor DNA, consistent with the suggestion that this represents a poor echinomycin binding site.

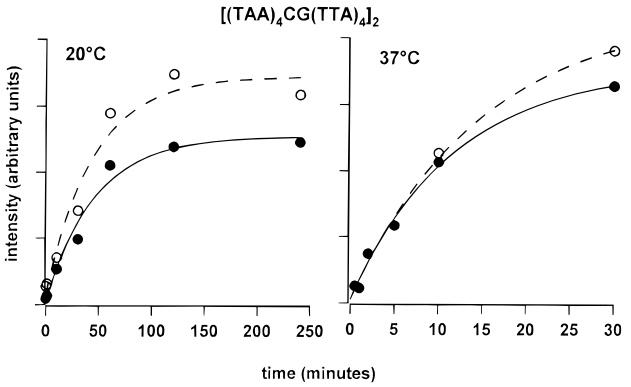

FIGURE 7: Rate of dissociation of echinomycin from $[(TAA)_4CG(TTA)_4]_2$ at 20 and 37 °C. The open circles correspond to upper the site, while the filled circles correspond to the lower site. The data are taken from densitometer scans of the autoradiographs presented in Figure 6. For each site, the intensity of the band corresponding to cleavage of the ApA step above the CpG (AACG) is compared with the cleavage of an ApA step at the center of the dimer, which is not affected by echinomycin binding. The points are fitted by single-exponential curves with the following decay constants: 20 °C, upper site 0.023 ± 0.006 min^{-1} (dashed curve), lower site 0.022 ± 0.005 min^{-1}; 37 °C, upper site 0.068 ± 0.013 min^{-1} (dashed curve), lower site 0.086 ± 0.015 min^{-1}.

CG Surrounded by $(CA)_n$·$(TG)_n$. Studies with actinomycin have suggested that GpC sites surrounded by $(AC)_n$·$(GT)_n$ present unusually good binding sites (Waterloh & Fox, 1992). We therefore have examined the dissociation of echinomycin from a DNA fragment containing a dimeric insert of $(CA)_5CG(TG)_5$. The results are presented in Figure 8. Echinomycin produces clear DNase I footprints around both CpG sites, which extend over about 7−8 base pairs. It can be seen that dissociation from these sites occurs very slowly upon adding the competitor DNA; bands within the footprints begin to reappear after 10−20 min at 20 °C and after 2−5 min at 37 °C. Quantitative analyses of these dissociation profiles are presented in Figure 9, yielding average dissociation rate constants of 0.061 and 0.26 min^{-1} at 20 and 37 °C, respectively. These values, which are included in the summary presented in Table 1, are about 4-fold faster than

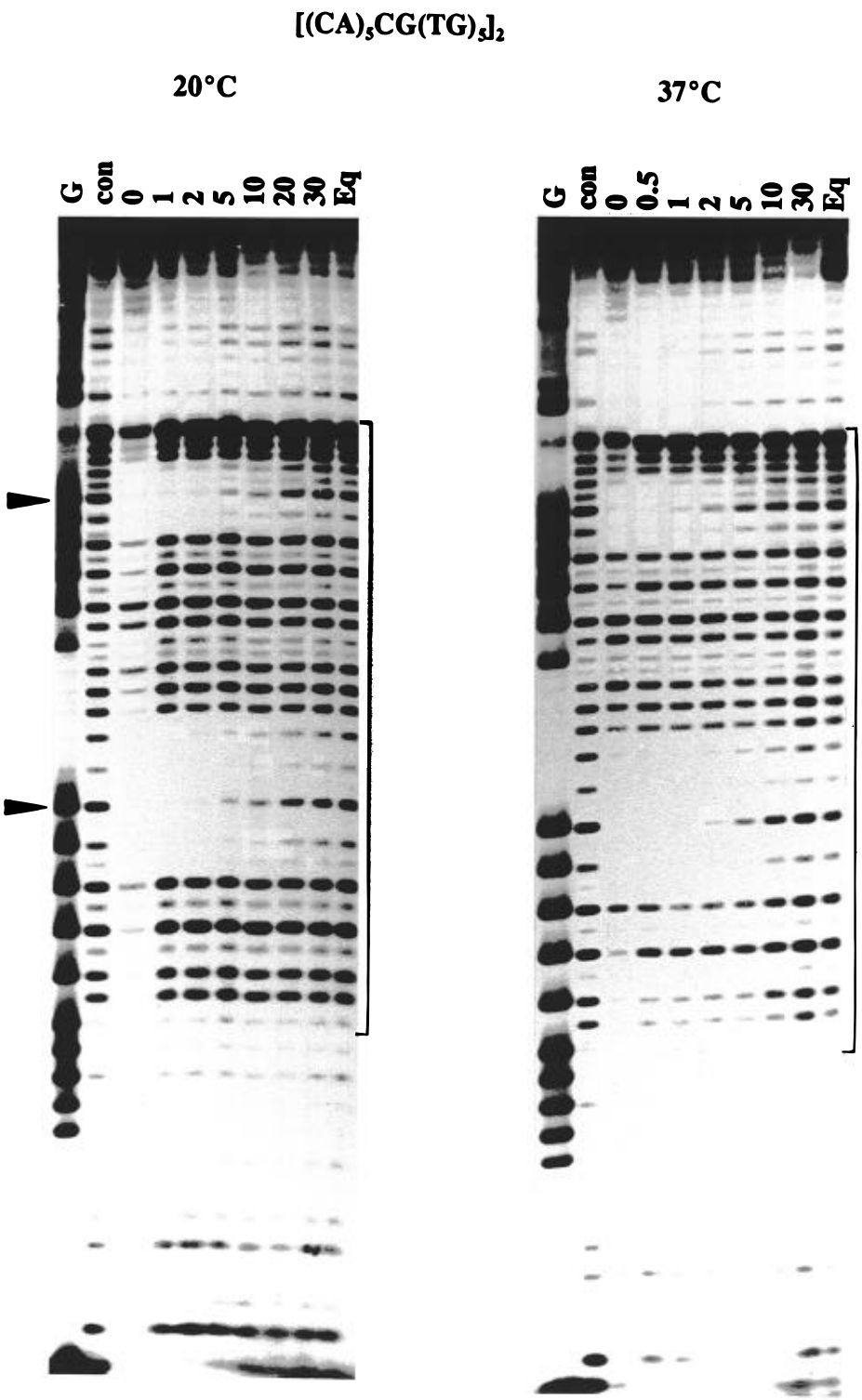

FIGURE 8: DNase I digestion patterns showing the dissociation of 20 μM echinomycin from a DNA fragment containing the dimeric insert $[(CA)_5CG(TG)_5]_2$ measured at 20 and 37 °C. The time after adding the competitor DNA (minutes) is indicated at the top of each lane. con indicates digestion of the DNA alone in the absence of any ligand; 0 corresponds to digestion of a complex with 20 μM echinomycin before adding the unlabeled DNA. In the track labeled Eq, the labeled and unlabeled DNAs were mixed before adding the ligand and represent the true equilibrium distribution of the ligand in the dissociating mixture. Tracks labeled G are Maxam−Gilbert dimethyl sulfate−piperidine markers specific for guanine. The arrows indicate the position of the guanines in the CpG sites; the square brackets show the position and length of the insert. Bands toward the top of the insert are compressed as a result of the high GC content of this DNA.

those estimated for the dissociation from $(TA)_5CG(TA)_5$. It therefore appears that, unlike actinomycin, echinomycin binding sites flanked by $(CA)_n{\cdot}(TG)_n$ are not especially strong.

Other CG Sites. We have also examined the binding of echinomycin to the sequences $(AT)_{10}CCCG(AT)_{10}$, $(AT)_{10}$-$CCGC(AT)_{10}$, and $(AT)_{10}CGGC(AT)_{10}$ containing the echinomycin binding tetranucleotides CCGA, CCGC, and TCGG respectively. The results are presented in Figure 10. As a result of the poor DNase I cleavage at the center of these inserts, echinomycin does not produce clear footprints with any of these fragments. However, changes can be seen in the ApT steps to the lower (3′) side of the CpG binding sites. Looking first at the central CCCG (left-hand panel), cleavage

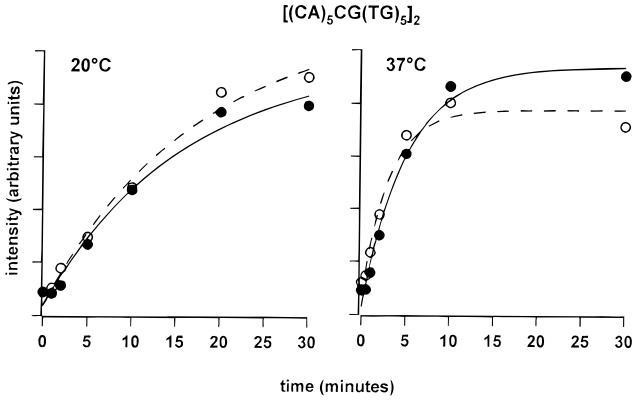

FIGURE 9: Rate of dissociation of echinomycin from $[(CA)_5CG(TG)_5]_2$ measured at 20 and 37 °C. The data are taken from densitometer scans of the autoradiographs presented in Figure 8. Filled circles correspond to the lower site, and open circles correspond to the upper site. For each site, the intensity of the band corresponding to cleavage of the central GpT step is compared with cleavage of the GpC step at the center of the dimer, which is not affected by echinomycin binding. The points are fitted by single-exponential curves with the following decay constants: 20 °C, upper site 0.059 ± 0.186 min^{-1} (dashed curve), lower site 0.064 ± 0.020 min^{-1}; 37 °C, upper site 0.32 ± 0.08 min^{-1} (dashed curve), lower site 0.199 ± 0.033 min^{-1}.

of the second ApT step below the central CG (i.e., CGATAT) is attenuated by echinomycin (the first ApT step is cut very poorly in the control in this sequence). This band rapidly reappears and has returned to the intensity in the control by 5−10 min. For CCGC (center panel), cleavage of the first ApT step below the CCGC is protected by echinomycin. This is still protected after 1 min, but is very similar to the intensity in the control after 5 min. In contrast, the dissociation from CGGC (right-hand panel) is slower. The first ApT step below the CGGC is protected by echinomycin, and this does not reappear until 10−30 min after adding the competitor DNA. Densitometric analysis of this autoradiograph yielded a dissociation rate constant of 0.087 ± 0.010 min^{-1} (Table 1).

These fragments also show an unusual cleavage pattern within the $(AT)_n$ tracts in the presence of echinomycin, as noted earlier with $T(AT)_8CG(AT)_{15}$ and as previously described (Fox *et al.*, 1991). This has disappeared by the first time point, consistent with the suggestion that it represents a much faster dissociating species.

DISCUSSION

The results presented in this paper confirm that echinomycin slowly dissociates from CpG sites in DNA with half-lives in the range 1−40 min at 20 °C. In addition, the dissociation is not the same from each CpG site and varies according to the surrounding sequences.

Comparison with SDS Sequestration. Early studies using SDS sequestration techniques, performed before the preference of echinomycin for CpG was firmly established, demonstrated that the dissociation of echinomycin from mixed-sequence DNA is a complex reaction requiring at least three exponentials for its complete description (Fox *et al.*, 1981). The results presented in this paper confirm that the complex dissociation profile observed with natural DNAs using SDS sequestration arises from parallel and not sequential dissociation processes. In addition, these results provide clear evidence that echinomycin dissociates from its individual binding sites in polymeric DNA in a single-step reaction. Since echinomycin has a staple-like structure, this implies that both chromophores dissociate simultaneously.

Although the precise values for each of the time constants estimated by SDS sequestration varied according to the ratio of ligand to DNA, the average values were about 20, 50, and 300 s, measured at 20 °C. In contrast, the dissociation from synthetic DNA was completely described by a single exponential with time constants of 80 and 25 s for poly(dG−dC) and poly(dA−dT), respectively. How do these values compare with the dissociation rates measured by DNase I footprinting in the present study? The dissociation times that we observed at 20 °C vary between about 35 min for $(TA)_5CG(TA)_5$ and $(TAA)_4CG(TTA)_4$ and less than 3 min for $T_{15}CGA_{15}$. The slowest time constant, measured by SDS sequestration, therefore is faster than the slowest dissociation rate seen with DNase I footprinting. However, it should be remembered that SDS contributes toward the ionic strength in the sequestration experiments and that 2% corresponds to $I = 0.1$. Increasing the ionic strength is known to decrease the binding constant of echinomycin to DNA (Wakelin & Waring, 1976), so that the values measured by footprinting (for which $I = 0.01$) necessarily should be slower. Indeed footprinting experiments with mixed-sequence DNAs (not shown) reveal that the rate of dissociation is increased in the presence of elevated ionic strength. Since we have shown that the dissociation of echinomycin from each CpG site can vary by an order of magnitude depending on the surrounding sequences, it seems that the slowest time constant in the SDS dissociation profiles represents only a subset of the available CpG sites. This probably corresponds to sites similar to those that show the slowest dissociation, as measured by footprinting. The faster two components must correspond to weaker CpG sites, as well as to other non-CG sites.

Preferred Binding Sites. The results presented in this paper demonstrate that the rate of dissociation of echinomycin from CpG sites depends on the nature of the flanking sequences. For sites flanked by $(AT)_n$, dissociation from ACGT is slower than from TCGA. We can suggest several reasons for this difference. Firstly, it is known that alternating purines and pyrimidines possess an unusual structure, in which it is thought that, in the case of $(AT)_n$, the YpR step is underwound. This may render the RpY steps particularly good sites into which the quinoxaline chromophores can be intercalated. An alternative explanation may be related to the ability of ACGT and TCGA to adopt distorted conformations. NMR studies have shown that the surrounding AT bases can adopt a Hoogsteen configuration in ACGT but not TCGA (Gao & Patel, 1989; Gilbert & Feigon, 1991). Although it is thought that Hoogsteen base pairs do not form in longer DNA molecules in solution, these unusual conformations may reflect the inherent deformability of each sequence, which may aid or hinder echinomycin binding. An alternative explanation may be derived from computational studies on the interaction of echinomycin with TCGA and ACGT (Gallego *et al.*, 1993, 1994). Hoogsteen base pair formation alters the dipole moment of an AT base pair; this arrangement improves the base stacking interactions of echinomycin with ACGT, but leads to unfavorable dipolar interactions with TCGA.

Since echinomycin does not produce DNase I footprints with $A_{15}CGT_{15}$ or $T_{15}CGA_{15}$, it is not possible to compare

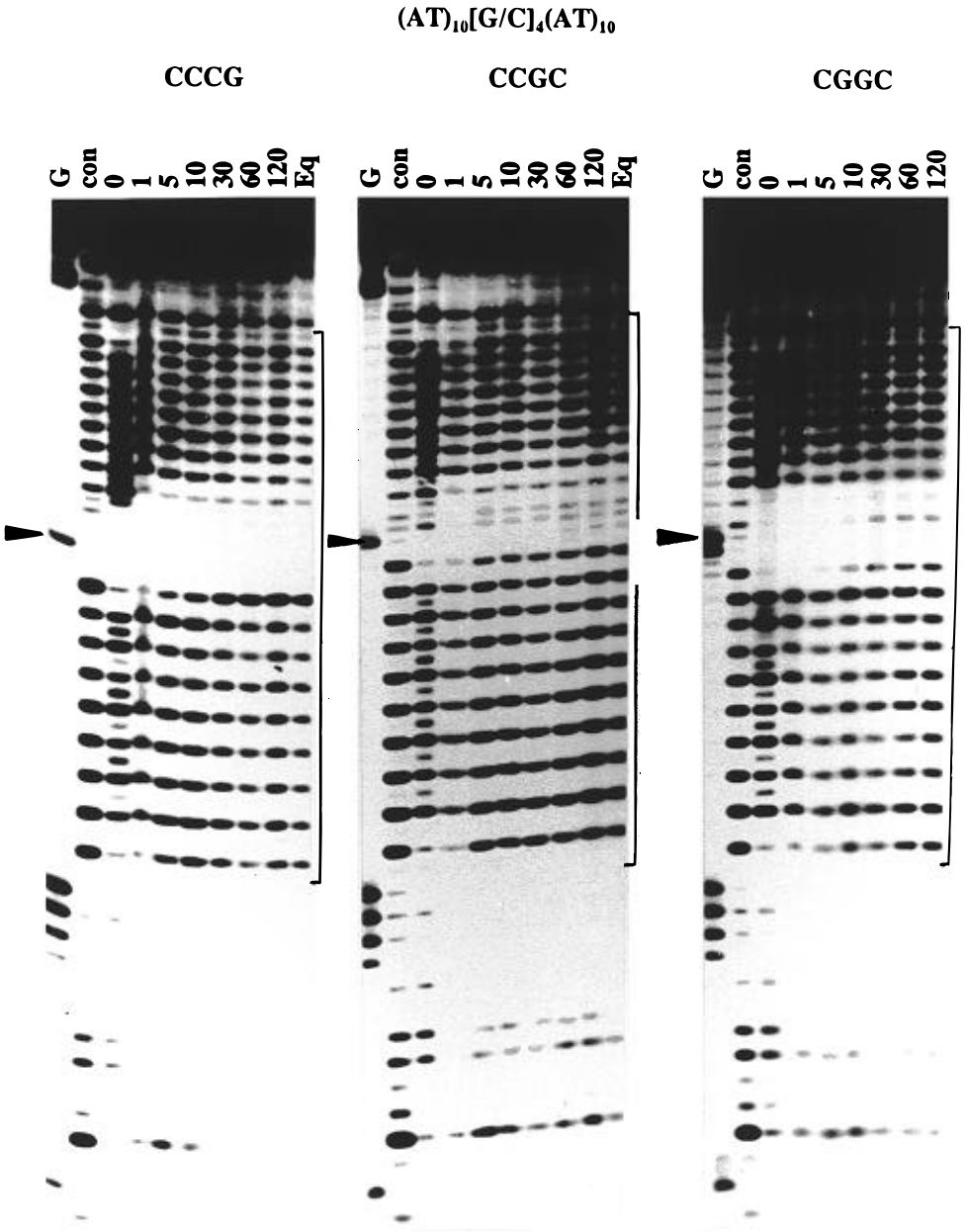

FIGURE 10: DNase I digestion patterns showing the dissociation of echinomycin from DNA fragments containing the inserts $(AT)_{10}$CCCG-$(AT)_{10}$, $(AT)_{10}$CCGC$(AT)_{10}$, and $(AT)_{10}$CGGC$(AT)_{10}$, measured at 20 °C. Aliquots were removed from each mixture at various times after adding the unlabeled calf thymus DNA and subjected to short (12 s) digestion by DNase I. The time after adding the competitor DNA (minutes) is indicated at the top of each lane. con indicates digestion of the DNA alone in the absence of any ligand; 0 corresponds to digestion of a complex with 20 μM echinomycin before adding the unlabeled DNA. In the tracks labeled Eq, the labeled and unlabeled DNAs were mixed before adding the ligand and represent the true equilibrium distribution of the ligand in the dissociating mixture. Tracks labeled G correspond to Maxam−Gilbert dimethyl sulfate−piperidine markers specific for guanine. The arrows indicate the position of the guanines in each GpC site; the square brackets show the position and length of the inserts.

TCGA and ACGT when they are surrounded by A_n·T_n rather than $(AT)_n$. However, echinomycin-induced hyperreactivity to diethyl pyrocarbonate with $T_{15}CGA_{15}$ disappears with a half-life of about 3 min, consistent with the suggestion that dissociation from CpG surrounded by A_n·T_n is much faster than that from $(AT)_n$. This difference is even more striking when we consider that diethyl pyrocarbonate appears to underestimate the rate of dissociation compared with DNase I. Indeed, Figure 4 confirms that echinomycin dissociates much faster from $T_{15}CGA_{15}$ than from $T(AT)_8CG(AT)_{15}$, even though both sequences possess the same central tetranucleotide (TCGA). The apparent difference between the values obtained with DNase I and diethyl pyrocarbonate with $T(AT)_8CG(AT)_{15}$ is puzzling, but may be related to the different ways in which these two probes function. Changes in diethyl pyrocarbonate reactivity represent a positive footprint against a weak background and, therefore, may be apparent at low levels of occupancy, in contrast to DNase I, which may require much higher levels of occupancy to significantly decrease band intensity. It is also possible, although unlikely, that the DNA structural changes detected by diethyl pyrocarbonate are relatively long-lived and persist after the ligand has dissociated. Whatever the origin of the difference between these two probes it is entirely consistent with previous observations that enhancements in diethyl pyrocarbonate reactivity appear at lower ligand concentrations than DNase I footprints (Portugal *et al.*, 1988; Fox *et al.*, 1991).

The faster dissociation from TCGA than from ACGT is also apparent with $(ATT)_4CG(AAT)_4$ and $(TAA)_4CG(TTA)_4$. Dissociation from the former is very fast, while the latter represents one of the slowest dissociating species. The dissociation from $(TAA)_4CG(TTA)_4$ is less sensitive to changes in temperature than many of the other sequences studied. Although there could be several possible explanations for this difference, we favor the suggestion that this is related to the observation that poly(dA)·poly(dT) melts at a higher temperature than poly(dA−dT) (Riley *et al.*, 1966). If dissociation is accompanied by local DNA breathing, then more stable sequences should display slower dissociation rates.

Dissociation from $(CA)_5CG(TG)_5$ is faster than from $(TA)_5CG(TA)_5$ at 20 °C, even though both contain the central tetranucleotide ACGT located within a block of alternating purines and pyrimidines. This contrasts with actinomycin for which it has been suggested that flanking $(AC)_n$·$(GT)_n$ potentiates binding (Waterloh & Fox, 1992). At 37 °C the rate of dissociation from these sequences is very similar. This is again consistent with the suggestion that sequences with a lower melting temperature [$(TA)_5CG(TA)_5$, on account of its higher AT content] are more sensitive to changes in temperature.

The data presented in Figure 10 show that dissociation from $(AT)_{10}CGGC(AT)_{10}$ is slower than that from $(AT)_{10}$-$CCCG(AT)_{10}$ and $(AT)_{10}CCGC(AT)_{10}$. Since the first two contain the same central tetranucleotide binding site (TCGG/CCGA), this difference cannot be solely due to changes in the binding sites and must reflect longer range differences in DNA structure or flexibility. In this regard it may be significant that the weaker site is preceded by a block of pyrimidines (TCCCGATA), in contrast to the stronger site, which is located within a region that more closely resembles alternating purines and pyrimidines (TATCGGCA).

It should be remembered that slower dissociation times do not necessarily mean stronger binding sites. It may be that the sequences from which the ligand dissociates more slowly are also sites to which the rate of association is also correspondingly slow.

Secondary Binding Sites. Several studies have shown that echinomycin is capable of binding to other sequences as well as CpG, albeit with lower affinity. Binding isotherms demonstrated that echinomycin binds to poly(dA−dT) with a binding constant of 0.3 μM^{-1}, compared with 0.7 μM^{-1} to poly(dG−dC) (Wakelin & Waring, 1976). Dissociation from poly(dA−dT) is also slow with a half-life of 25 s (Fox *et al*., 1981). Previous studies have also shown that although footprints are observed only around CpG steps, surrounding regions of $(AT)_n$ exhibit an unusual cleavage pattern in the presence of the antibiotic (Fox & Kentebe, 1990b; Waterloh & Fox, 1991; Fox *et al*., 1991), consistent with a weaker interaction with ApT. This pattern can be seen in the time 0 lanes of Figures 3 and 10, but disappears rapidly upon adding the competitor DNA in contrast to the footprints at the central CpG sites, which persist for much longer. Since these changes are no longer evident at the first time point (30 s), this must be the upper limit for the dissociation time from the ApT sites. Comparison with the SDS sequestration data for poly(dA−dT) would lead us to expect a slower dissociation time at the lower ionic strength used in the footprinting experiments. This suggests that the binding to $(AT)_n$ does not show the same salt dependence as other sequences and may indicate that it occurs by a different mechanism (nonintercalative?).

Biological Implications. It is thought that the cytotoxic activity of echinomycin, together with other DNA binding antibiotics, arises from inhibition of RNA polymerase and that the efficacy of this action depends on the lifetime of the complex (Wilson & Jones, 1981). The results of our kinetic analysis suggest that not all CpG sites are equipotent biological targets for echinomycin. This may be especially relevant since the CpG dinucleotide step is underrepresented in the human genome. Those sites from which the ligand dissociates slowly are more likely to cause the termination of transcription, rather than the simple pause of RNA polymerase (White & Phillips, 1989a; Phillips *et al*., 1990).

REFERENCES

Addess, K. J., & Feigon, J. (1994*a*) *Biochemistry 33*, 12397−12404.

Addess, K. J., & Feigon, J. (1994*b*) *Nucleic Acids Res. 22*, 5484−5491.

Bailly, C., & Waring, M. J. (1995) *Nucleic Acids Res. 23*, 885−892.

Bailly, C., Marchand, C., & Waring, M. J. (1993) *J. Am. Chem. Soc. 115*, 3784−3785.

Bailly, C., Gentle, D., Hamy, F., Purcell, M., & Waring, M. J. (1994) *Biochem. J. 300*, 165−173

Carpenter, M. L., Marks, J. N., & Fox, K. R. (1993) *Eur. J. Biochem. 215*, 561−566.

Chen, F.-M. (1988*a*) *Biochemistry 27*, 1843−1848.

Chen, F.-M. (1988*b*) *Biochemistry 27*, 6393−6397.

Chen, F.-M. (1990) *Biochemistry 29*, 7684−7690.

Chen, F.-M. (1992) *Biochemistry 31*, 6223−6228.

Fletcher, M. C., & Fox, K. R. (1993) *Nucleic Acids Res. 21*, 1339−1344.

Fletcher, M. C., Olsen, R. K., & Fox, K. R. (1995) *Biochem. J. 306*, 15−19.

Fox, K. R., & Waring, M. J. (1981) *Biochim. Biophys. Acta 654*, 279−286.

Fox, K. R., & Kentebe, E. (1990*a*) *Biochem. J. 269*, 217−221.

Fox, K. R., & Kentebe, E. (1990*b*) *Nucleic Acids Res. 18*, 1957−1963.

Fox, K. R., Wakelin, L. P. G., & Waring, M. J. (1981) *Biochemistry 20*, 5768−5779.

Fox, K. R., Marks, J. N., & Waterloh, K. (1991) *Nucleic Acids Res. 19*, 6725−6730.

Gallego, J., Ortiz, A. R., & Gago, F. (1993) *J. Med. Chem. 36*, 1548−1561.

Gallego, J., Luque, F. J., Orozco, M., Burgos, C., Builla-Alvarez, J., Rodrigo, M. M., & Gago, F. (1994) *J. Med. Chem. 37*, 1602−1609.

Gao, X., & Patel, D. J. (1988) *Biochemistry 27*, 1744−1751.

Gilbert, D. A., & Feigon, J. (1991) *Biochemistry 30*, 2483−2494.

Gilbert, D. A., & Feigon, J. (1992) *Nucleic Acids Res. 20*, 2411−2420.

Gilbert, D. A., van der Marel, G. A., van Boom, J. H., & Feigon, J. (1989) *Proc. Natl. Acad. Sci. U.S.A. 86*, 3006−3010.

Leroy, J. L., Gao, X., Misra, V., Gueron, M., & Patel, D. J. (1992) *Biochemistry 31*, 1407−1415.

Low, C. M. L., Drew, H. R., & Waring, M. J. (1984) *Nucleic Acids Res. 12*, 4865−4879.

Marchand, C., Bailly, C., McLean, M. J., Moroney, S. E., & Waring, M. J. (1992) *Nucleic Acids Res. 20*, 5601−5601.

McLean, M. J., & Waring, M. J. (1988) *J. Mol. Recog. 1*, 138−151.

Phillips, D. R., White, R. J., Dean, D., & Crother, D. M. (1990) *Biochemistry 29*, 4812−4819.

Portugal, J., Fox, K. R., Mclean, M. J., Richenberg, J. L., & Waring, M. J. (1988) *Nucleic Acids Res. 16*, 3655−3670.

Quigley, G. J., Ughetto, G., van der Marel, G. A., van Boom, J. H., Wang, A. H.-J., & Rich, A. (1986) *Science 232*, 1255−1258.

Riley, M., Maling, B., & Chamberlain, M. J. (1966) *J. Mol. Biol. 20*, 359−389.
Sayers, E. W., & Waring, M. J. (1993) *Biochemistry 32*, 9094−9107.
Ughetto, G., Wang, A. H.-J., Quigley, G. J., van der Marel, G., van Boom, J. H., & Rich, A. (1985) *Nucleic Acids Res. 13*, 2305−2323.
Van Dyke, M. W., & Dervan, P. B. (1984) *Science 225*, 1122−1127.
Wakelin, L. P. G., & Waring, M. J. (1976) *Biochem. J. 157*, 721−740.
Wang, A. H.-J., Ughetto, G., Quigley, G. J., Hakoshima, T., van der Marel, G. A., van Boom, J. H., & Rich, A. (1984) *Science 225*, 1115−1121.
Wang, A. H.-J., Ughetto, G., Quigley, G. J., & Rich, A. (1986) *J. Biomol. Struct. Dyn. 4*, 319−342.
Waring, M. J. (1993) in *Molecular Aspects of Anticancer Drug-DNA Interactions* (Neidle, S., & Waring, M. J., Eds.) Vol. 1, pp 213−242, MacMillan, London.
Waring, M. J., & Bailly, C. (1994) *Gene 149*, 69−79.
Waterloh, K., & Fox, K. R. (1991) *Nucleic Acids Res. 19*, 6719−6724.
Waterloh, K., & Fox, K. R. (1992) *Biochim. Biophys. Acta* 1131, 300−306.
White, R. J., & Phillips, D. R. (1989a) *Biochemistry 28*, 4277−4283.
White, R. J., & Phillips, D. R. (1989b) *Biochemistry 28*, 6259−6269.
Wilson, D. W., & Jones, R. L. (1981) *Adv. Pharmacol. Chemother. 18*, 177−222.

BI9523623